International Journal of Global Affairs , Research and Development (IJGARD) Vol.3, No.2, 2025, 516-545, ISSN 2992-2488

COMPARING THE ACCURACY OF GOOGLE EARTH AND GLOBAL NAVIGATION SATELLITE SYSTEM'S (HI-TARGET GPS) IN TOPOGRAPHIC MAPPING

Rasheed, Y.O.,[1]* Ibrahim, M.M.,[2] and Matapa, I.J.[1]

[1]Department of Surveying and Geoinformatics, Nigerian Army University, Biu, Borno state, Nigeria
[2]Department of Surveying and Geoinformatics, Abubakar Tafawa Balewa University, Bauchi, Niger

*__Correspondence:__ rasheed.yusuf@naub.edu.ng; Tel: +234-806-936-3796

ABSTRACT

Google Earth provides freely accessible spatial data, making it attractive for quick and preliminary mapping. However, topographic and engineering projects require highly accurate coordinates to ensure proper design and accurate material costing. Therefore, this study investigates the accuracy of Google Earth in comparison with GNSS. The aim of the study is to compare the positional accuracy of Google Earth and GNSS in topographic mapping. The study was conducted at the Nigerian Army University Biu temporary site. GNSS coordinates were obtained using a Hi-target GPS receiver, while Google Earth data were sourced online through GPS Visualizer. Civil CAD 3D and ArcGIS Pro were used to generate the Digital Elevation Model (DEM), Triangulated Irregular Network (TIN), and contour maps for both datasets, while Excel was employed for statistical analysis. The results showed that the GNSS system was far more accurate for geodetic, engineering, and plane surveying, whereas Google Earth was suitable mainly for reconnaissance or small-scale surveys. A correlation coefficient of 0.701 was obtained between both datasets, with a mean height difference of 5.47 m and a standard deviation of 1.42 m. The study concludes that GNSS should be adopted where high accuracy is essential particularly in construction design, execution, and material quantification because it provides more reliable and up-to-date spatial data than Google Earth, which exhibited higher misclosures.

Keywords: GNSS (RTK), Google Earth, Topographical Mapping, DEM, TIN and Contour

1.0 INTRODUCTION

Google Earth offers easy and free access to spatial data, making it a popular alternative for rapid mapping and preliminary spatial analysis. However, for topographic and engineering projects that demand high precision, particularly for accurate design, earthwork estimation, and material costing, greater positional and vertical accuracy is essential.

Topographic surveying captures detailed three-dimensional information about terrain characteristics, including contours, elevations, and landforms. Such maps are critical for understanding landscape conditions and assessing suitability for infrastructure projects such as highways, bridges, and stormwater management systems (Olatunde et al., 2025; Sharma & Gupta, 2014). In structural construction, engineers rely on topographic data to evaluate ground stability and ensure foundations can withstand soil movement and settlement (International Hydrographic Organization, n.d.). Urban planners similarly use elevation data to design settlements that conform to natural terrain, protect flood-prone zones, and optimize land use planning (Fisher *et al*., 2010; BP Chaliha College, n.d.). Additionally, topographic information supports accurate estimation of excavation and backfill volumes, which directly influence construction costs and budgeting decisions (Open Topography, 2023). The extraction of elevation data from multiple sources, such as DEMs, TINs, and contour maps, further enables engineers and planners to evaluate terrain characteristics efficiently (Civil Engineering Journal Editorial Office, 2024; Sensors and Materials Editorial Office, 2023).

Achieving accurate elevation measurements remains challenging due to several sources of error. Instrument-related issues such as sensor misalignment, calibration errors, and signal interference can degrade data quality, while environmental conditions including rainfall, haze, and vegetation cover may obstruct observations (Orhan et al., 2023; Richard, 2017). Human factors, including surveyor fatigue, observational errors, and inconsistencies in field procedures, further contribute to inaccuracies, especially in rugged or densely vegetated terrain (TIU, 2021). These errors can propagate into digital terrain models, leading to inaccurate slope determination and inflated earthwork volume estimates (Mesbah, 2023; Open Topography, 2023).

Conventional surveying techniques, such as rod-and-level methods, remain highly reliable for precise height determination over short distances. Differential leveling, for instance, can achieve millimeter-level accuracy on relatively flat terrain, making it suitable for establishing benchmarks and control points ((American Society of Civil Engineers, 2003). Total stations, which integrate electronic distance measurement with precise angular observations, are capable of delivering sub-millimeter vertical accuracy under favorable conditions (Mettatec, 2023; Orhan et al., 2023). Despite their accuracy, these methods are often constrained by high equipment costs, extended field

durations, and logistical difficulties in areas with complex terrain or dense vegetation (TIU, 2021; Omona *et al.*, 2021).

Recent advancements in geospatial technology emphasize efficiency and coverage. Drone-based photogrammetry enables rapid acquisition of high-resolution imagery and generation of three-dimensional terrain models without extensive ground surveys (Civil Engineering Journal Editorial Office, 2024; Richard, 2017). Similarly, Real-Time Kinematic (RTK) GNSS provides centimeter-level positional accuracy, with horizontal accuracy of approximately 1–2 cm and vertical accuracy of 2–3 cm under ideal conditions, facilitating real-time production of DEMs, TINs, and contour maps without permanent ground control points (Botygina, N. (2025); Omona et al., 2021; TIU, 2021). Google Earth integrates elevation data primarily from the Shuttle Radar Topography Mission (SRTM) and aerial imagery, offering free and rapid access to global elevation information for reconnaissance and preliminary analysis (Guo et al., 2020; Benker et al., 2017). These modern approaches can reduce survey time by 70-90% compared to traditional methods, making them particularly valuable in remote or inaccessible regions (MES Innovation, 2022; Chigbu et al., 2019).

Nevertheless, each method presents inherent limitations. RTK GNSS performs optimally in open environments but may experience signal degradation due to obstructions such as buildings, trees, or multipath effects, resulting in centimeter-level errors (University of Baghdad, n.d.; Omona et al., 2021). Google Earth's positional accuracy varies spatially, with reported horizontal errors ranging from 0.04 to 2.64 m and vertical errors between 1.63 and 5.7 m globally (Benker et al., 2017; El-Ashmawy, 2024). While accuracy is generally higher on flat terrain, errors tend to increase in mountainous or forested regions where interpolation dominates the elevation model (Potuckova et al., 2020; Guo et al., 2020). Consequently, although Google Earth performs adequately for large-scale urban mapping at approximately 1:30,000 scale, its limitations may lead to earthwork volume errors of up to 20% in complex terrains (Sensors and Materials Editorial Office, 2023; Journal of Maps and Spatial Engineering, n.d.).

Direct comparative studies between Google Earth and RTK GNSS are essential, particularly for construction projects where inaccuracies in volume estimation can result in significant cost overruns. However, limited research exists that evaluates both datasets using consistent outputs such as DEMs with 1-5 m grid spacing, detailed TINs, and contour intervals of 0.5-1 m (Nigerian Journal of

Environmental Sciences and Technology, 2023; El-Ashmawy, 2024; Potuckova et al., 2020). Such comparisons typically assess RMSE, systematic bias, and spatial consistency across varying terrain conditions (Mesbah, S et al., 2023; Guo et al., 2020). Ultimately, the selection between Google Earth and GNSS techniques depends on project requirements and site characteristics: GNSS is better suited for areas with complex terrain or dense infrastructure, while Google Earth remains a practical, cost-free option for preliminary assessments and low-precision applications (Chigbu *et al*., 2019; MES Innovation, 2022; Guo *et al*., 2020).

The aim of this study is to compare the accuracy of Google Earth elevation data and GNSS for topographic mapping at the NAUB temporary site, while the justification lies on the fact that the availability of accurate elevation data is essential for successful topographic surveying, construction planning, and other geospatial applications. This study is important as it will provide insights into the reliability of Google Earth data for topographic mapping in the study area. By comparing it with high-precision GNSS data, this study will identify the extent of discrepancies, if any, and provide recommendations for the use of Google Earth DEM in similar environments. Furthermore, the findings from this study will benefit researchers, surveyors, engineers, and planners by highlighting the accuracy limitations and potential applications of Google Earth data. This will help improve the decision-making processes in construction, mapping, and land development projects

2.0 MATERIALS AND METHODS

2.1 Study Area

This research was conducted at the temporary campus site of the Nigerian Army University Biu (NAUB) shown in figure 1, located in Biu town, Borno State, northeastern Nigeria. The study area lies approximately between latitude 10°35′00″N and 10°36′00″N and longitude 12°11′00″E and 12°12′00″E, encompassing nearly eight hectares. This location was chosen due to the limited established geodetic control networks within the vicinity, providing a practical scenario to evaluate the height and positional accuracy of Google Earth data against ground-based GNSS measurements.

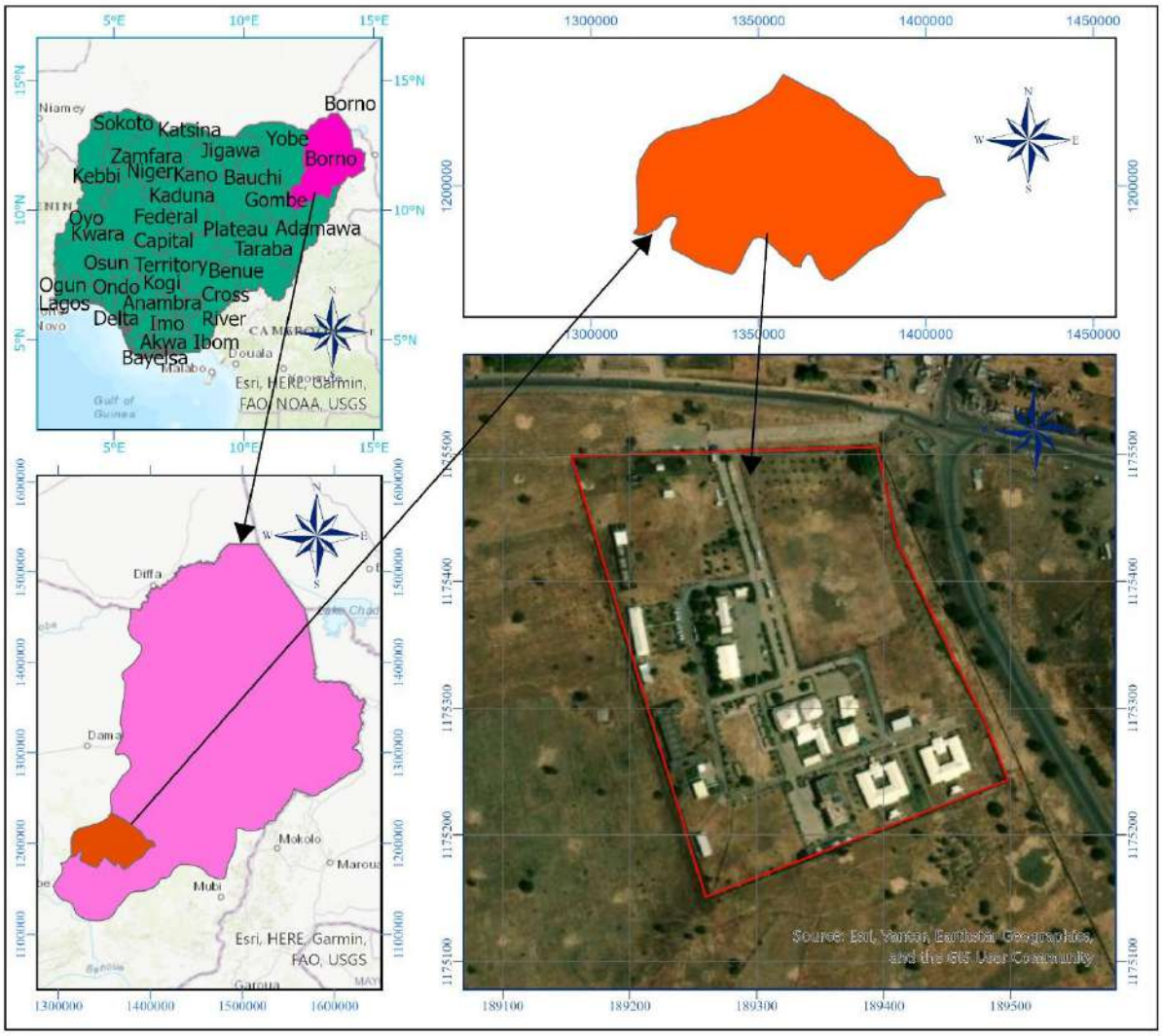

Figure 1: Map of study area

2.2 Materials

A combination of high-precision instruments, geospatial software, and online platforms were employed for data acquisition, processing, and analysis. These consisted of:

2.2.1 Instrument and Software

1. Hi-Target V30 GNSS Receiver: Utilized for acquiring static and real-time kinematic (RTK) measurements, providing ellipsoidal heights alongside horizontal coordinates.
2. Google Earth Pro: Used to extract the equivalent positional and elevation data for the grid points established within the study area.

3. GPS Visualizer (Web-Based Tool): Assisted in converting KML files obtained from Google Earth into UTM coordinates compatible with GNSS survey data.
4. AutoCAD Civil 3D (2019 version): Deployed to digitize project boundaries, generate a regular grid at 25-meter intervals, and export the resulting coordinate points.
5. ArcGIS Pro: Served in the spatial analysis, including the creation of digital elevation models (DEMs), triangulated irregular networks (TINs), and contour maps from both GNSS and Google Earth data.
6. Microsoft Excel: Applied for conducting statistical analyses encompassing mean error, standard deviation, root mean square error (RMSE), Pearson correlation coefficients, as well as charting and graphical representation.
7. Geoid Model (EGM96/EGM2008): Enabled height conversion from GNSS ellipsoidal elevations to orthometric heights, facilitating direct comparison with Google Earth data.

2.2.3 Data and their sources

This study utilized both primary and secondary datasets to assess the accuracy of Google Earth elevation data in comparison with GNSS RTK measurements at the NAUB Temporary Site. The datasets used and their respective sources are presented in Table 1.

Table 1: Datasets Used and Their Sources

S/N	Dataset / Tool	Source
1	GNSS RTK Survey Data	Field survey using Hi-Target V30 GNSS Receiver
2	Google earth coordinates (KML data)	Google Earth Pro
3	Google Earth Elevation	GPS Visualizer (web-based tool)
4	Project Boundary and Grid Data	AutoCAD Civil 3D (2019 version)
5	Spatial Analysis Outputs (DEM, TIN, Contours)	ArcGIS Pro
6	Orthometric Height Data	Geoid Model (EGM96 / EGM2008)
7	Statistical Analysis Results	Microsoft Excel

2.3 Methodology

Figure 2 shows flowchart of the methodology adopted in this research, a beginning with study area identification and boundary digitization in Google Earth Pro. It proceeded through KML export to civil 3D for grid generation at 25 m intervals, control point establishment via static GNSS and AUSPOS, RTK verification, and GNSS data collection at 72 grid nodes. Subsequent steps cover Google Earth extraction for matching nodes, UTM transformation using GPS Visualizer, ellipsoidal-to-orthometric height conversion with EGM96/EGM2008 geoid, and import into ArcGIS Pro for DEM (Kriging), TIN, 0.5 m contours, and vertical difference mapping. The process concludes with Excel-based statistical analysis (mean error, SD, RMSE, R-value) and quality validation

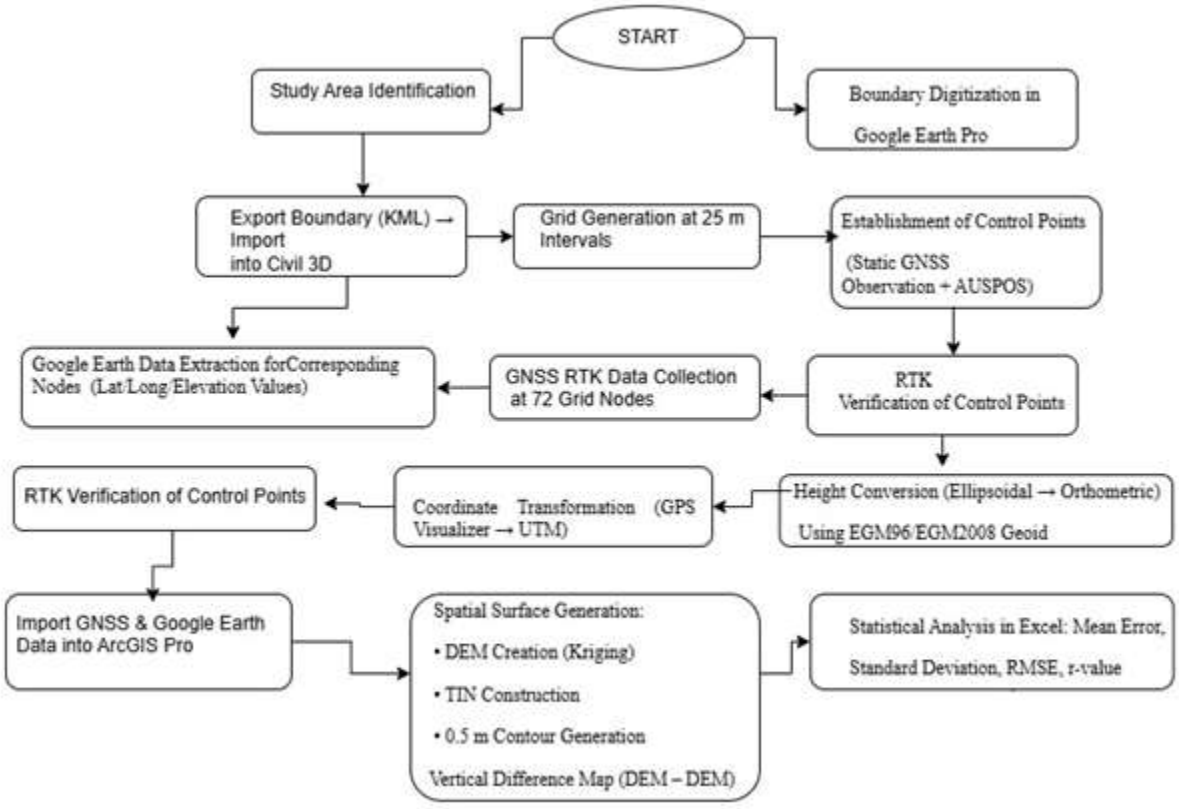

Figure 2: Flowchart of the methodology

2.3.1 Boundary Digitization and Grid Generation

The study commenced by digitizing the project perimeter within Google Earth Pro. The polygon representing the site boundary was exported as a KML format file and subsequently imported into

civil 3D software, where it was redrawn and subdivided into a grid with 25-meter spacing. This process resulted in 72 intersection points across the site, each uniquely labeled (NAUB_01 through NAUB_72), strategically distributed to capture the spatial variability of terrain including developed and undeveloped zones.

2.3.2 Control Point Establishment

Due to inadequate existing geodetic controls within the area, three new control points were established. Static GNSS observations were conducted using the Hi-Target V30 receiver for 12 hours per station, over three consecutive days. The raw observational files in RINEX format were submitted to the Australian AUSPOS service for processing, yielding high-accuracy WGS84 horizontal coordinates and ellipsoidal heights.

Subsequently, the same points were monitored in RTK mode to confirm consistency. The mean positional difference between static and RTK solutions was found to be 2.5 cm, which meets the precision requirements for third-order survey standards.

Table 2: Control Point Positions - Comparison of Static and RTK Measurements

	STATIC OBSERVATION			RTK OBSERVATION			DIFFERENCE IN OBSERVATION		
station	Northing(m)	Easting(m)	Height(m)	Northing(m)	Easting(m)	Height(m)	Diff(N_m)	Diff(E_m)	Diff(H_m)
SUR/18U/05	1174813.097	189261.495	711.025	1174813.127	189261.515	711.093	-0.03	-0.02	-0.068
SUR/18U/06	1174807.177	188957.679	708.049	1174807.208	188957.648	708.159	-0.031	0.031	-0.11
SUR/18U/07	1174628.947	189156.895	707.542	1174628.993	189156.873	707.591	-0.046	0.022	-0.049

2.3.3 GNSS Data Acquisition at Grid Nodes

After confirming the accuracy of the control points established in the field, (RTK) surveys were implemented across 72 grid nodes evenly distributed within the study area. At each node, a high-precision GNSS receiver recorded geospatial coordinates, including Easting, Northing, and Ellipsoidal Height (h). To ensure reliability and superior accuracy, only "Fixed" RTK solutions were accepted, which denote the highest confidence in the positional data by eliminating ambiguous float solutions. This rigorous approach reflects the critical need for precise ground truth data in spatial accuracy assessments. The final collection of GNSS data serves as the definitive reference dataset for comparison against coordinates derived from Google Earth imagery.

2.3.4 Google Earth Coordinate Extraction and Transformation

For comparative analysis, the same 72 nodes were located within Google Earth, where their latitude and longitude coordinates were extracted using KML export functionality. These raw geographic coordinates were then processed through the GPS Visualizer online tool to convert them into (UTM) Easting, Northing, and elevation values. This coordinate transformation ensures the datasets are directly comparable within the same projection and coordinate system framework. The resulting Google Earth-based dataset of XYZ coordinates aligns spatially with the GNSS data, facilitating detailed evaluation of positional accuracy, error quantification, and spatial agreement between the two data sources.

2.3.5 Height System Unification

To align the vertical reference systems, GNSS ellipsoidal heights were transformed into orthometric heights using the EGM96 or EGM2008 geoid model, since Google Earth reports elevations relative to mean sea level. This essential step created consistent datum references across both datasets prior to any comparative analysis. Orthometric heights better reflect practical terrain elevations, avoiding systematic vertical discrepancies that could skew accuracy evaluations.

2.3.6 Spatial Model Development and Visualization

The GNSS and Google Earth elevation datasets were first imported into the ArcGIS Pro environment and converted into geodatabase feature classes to ensure compatibility with spatial analysis tools. After verifying the coordinate system and projecting the datasets into a common spatial reference, the elevation points from each source were interpolated to create Digital Elevation Models (DEMs) using the raster to topo and kringing tools for smooth surface generation. The same point datasets were subsequently used to build Triangulated Irregular Networks (TINs) through the *created* TIN geoprocessing tool, which provided a detailed representation of break lines and terrain variability. From the DEMs, 0.5-meter interval contour lines were generated using the *contour* tool in the Spatial Analyst toolbox, ensuring terrain gradients and slope transitions were clearly visualized. To assess elevation discrepancies between the GNSS-derived and Google Earth-derived surfaces, raster algebra was performed using the Raster Calculator to subtract one DEM from the other, producing a vertical difference map that highlighted areas of elevation agreement or mismatch across the study area.

2.3.7 Data Extraction and Processing

Corresponding elevations for each control point were extracted from Google Earth using GPS Visualizer, a tool that allows users to obtain elevation data based on geographic coordinates. This process involved in putting the easting and northing coordinates into the tool to retrieve the associated Google Earth heights as shown in table 3.

Table 3: Coordinates from field surveyed (GNSS) and it's corresponded from GPS visualizer

S/No	Easting(m)	Northing(m)	GPS Height(m)	Google Earth Height(m)	Height-Diff (m)
1	189194.1868	1175406.155	720.702	717.3	3.402
2	189185.2276	1175429.495	720.4367	717.5	2.9367
3	189307.1183	1175181.719	722.3059	716.2	6.1059
4	189298.1591	1175205.059	722.2542	715.3	6.9542
5	189289.1999	1175228.398	722.4518	714.8	7.6518

Author's field data 2025

2.4 Statistical Analyses

In Microsoft Excel, the GNSS and Google Earth elevation values were arranged in paired columns to enable direct comparison of corresponding points. The height difference (Δh) for each observation was computed by subtracting the Google Earth elevation from the GNSS elevation, expressed as in equation 1.

$$\Delta h = h_{GNSS} - h_{GE}, \ldots\ldots\ldots\ldots\ldots\ldots\ldots\ldots\ldots\ldots\ldots\ldots\ldots\ldots\ldots\ldots\ldots\ldots\ldots\ldots (1)$$

Where: Δh = height difference, h_{GNSS} = GNSS elevation $_{GE}$ = Google Earth elevation. Following this, descriptive and inferential statistical analyses were performed. Using built-in Excel functions, the mean error (ME) was calculated to quantify the average deviation between the two datasets, while the standard deviation (SD**)** and range were used to describe the dispersion and variability of the height differences. The Root Mean Square Error (RMSE) as in equation 2 was computed to evaluate the overall vertical accuracy of Google Earth data relative to GNSS observations,

$$\text{RMSE} = \text{SQRT}\left(\left(\frac{1}{n}\right) * \Sigma(\Delta h_i^2)\right) \quad \text{..... (2)}$$

Where n is the number of obversions and Δh is the difference between the heights. Furthermore, Pearson's correlation coefficient (r) was determined to measure the strength and direction of the linear relationship between GNSS and Google Earth elevation values, expressed in equation 3 as

$$r = \frac{\Sigma[(h_{GNSS} - \bar{h}_{GNSS})(h_{GE} - \bar{h}_{GE})]}{\sqrt{[\Sigma(h_{GNSS} - \bar{h}_{GNSS})^2 \times \Sigma(h_{GE} - \bar{h}_{GE})^2]}}]). \quad \text{..... (3)}$$

The Pearson correlation coefficient (r) is used to assess the linear relationship between heights obtained from GNSS and those derived from Google Earth. In the equation, h_{GNSS} and h_{GE} are individual height values from GNSS and Google Earth, while $\bar{h}_{GNSS}$ and $\bar{h}_{GE}$ represent their mean values. The numerator describes the covariance between the two datasets, and the denominator scales this value using the standard deviations of both height sets. The value of r ranges from −1 to +1 and indicates the strength and direction of the linear relationship between the two height datasets.

For clarity, a summary table was prepared to present all statistical metrics alongside their computed values. In addition, scatter plots were generated to visually assess the correlation pattern between the two datasets and to identify potential outliers or inconsistencies that could influence the accuracy assessment.

2.4.1 Data Quality and Validation Procedures

To ensure the accuracy, consistency, and overall reliability of the survey datasets, a series of coordinated data quality and validation procedures were undertaken throughout the workflow. Static GNSS observations were processed through the AUSPOS online service, which refined positional estimates and ensured georeferencing precision remained within acceptable tolerances. The integrity of the control network was further validated through real-time kinematic (RTK) checks, where repeated observations confirmed minimal positional deviations. To maintain positional consistency across data sources, the coordinates obtained from GNSS were cross-verified against corresponding Google Earth values, allowing any notable discrepancies to be flagged for further review. The spatial grid design also contributed to data quality, as the density and uniform distribution of grid points allowed sufficient capture of terrain variability while reducing sampling bias. A unified vertical

reference system was adopted to eliminate potential datum inconsistencies between datasets, ensuring comparability of elevation values. Finally, the combination of spatial analysis in ArcGIS Pro and statistical evaluations in Microsoft Excel provided a rigorous framework that strengthened the robustness and credibility of the study's findings.

3.0 RESULTS AND DISCUSSION

This section presents a detailed analysis comparing elevation data obtained from Google Earth and a Hi-Target GNSS system. The objective is to assess the accuracy of Google Earth-derived elevations for topographic mapping by comparing them with high-precision GNSS measurements. The analysis for data visualization and interpretation as shown in figure 3.

3.1 Data Compilation

The collected data were compiled into a CSV file with the following structure as shown in table 4.

Table 4: Sample of Data used

S/NO	Easting(m)	Northing (m)	GPS Height (m)	Google Earth Height (m)
1	189194.1868	1175406.155	716.702	717.3
2	189185.2276	1175429.495	716.4367	717.5
3	189307.1183	1175181.719	718.3059	716.2
4	189298.1591	1175205.059	718.2542	715.3
5	189289.1999	1175228.398	718.4518	714.8
6	189280.2407	1175251.738	718.7372	716
7	189271.2815	1175275.077	718.9305	717.8
8	189262.3223	1175298.417	719.0196	718.7
9	189253.3631	1175321.756	718.8744	718
10	189244.4039	1175345.096	718.6091	717.2

Authors field data 2025

3.1.1 Boundary Digitization and Grid Generation

The study commenced by digitizing the project perimeter within Google Earth Pro. The polygon representing the site boundary was exported as a KML format file and subsequently imported into civil 3D software, where it was redrawn and subdivided into a grid with 25-meter spacing. This process resulted in 72 intersection points across the site, each uniquely labeled (NAUB_01 through NAUB_72), strategically distributed to capture the spatial variability of terrain including developed and undeveloped zones.

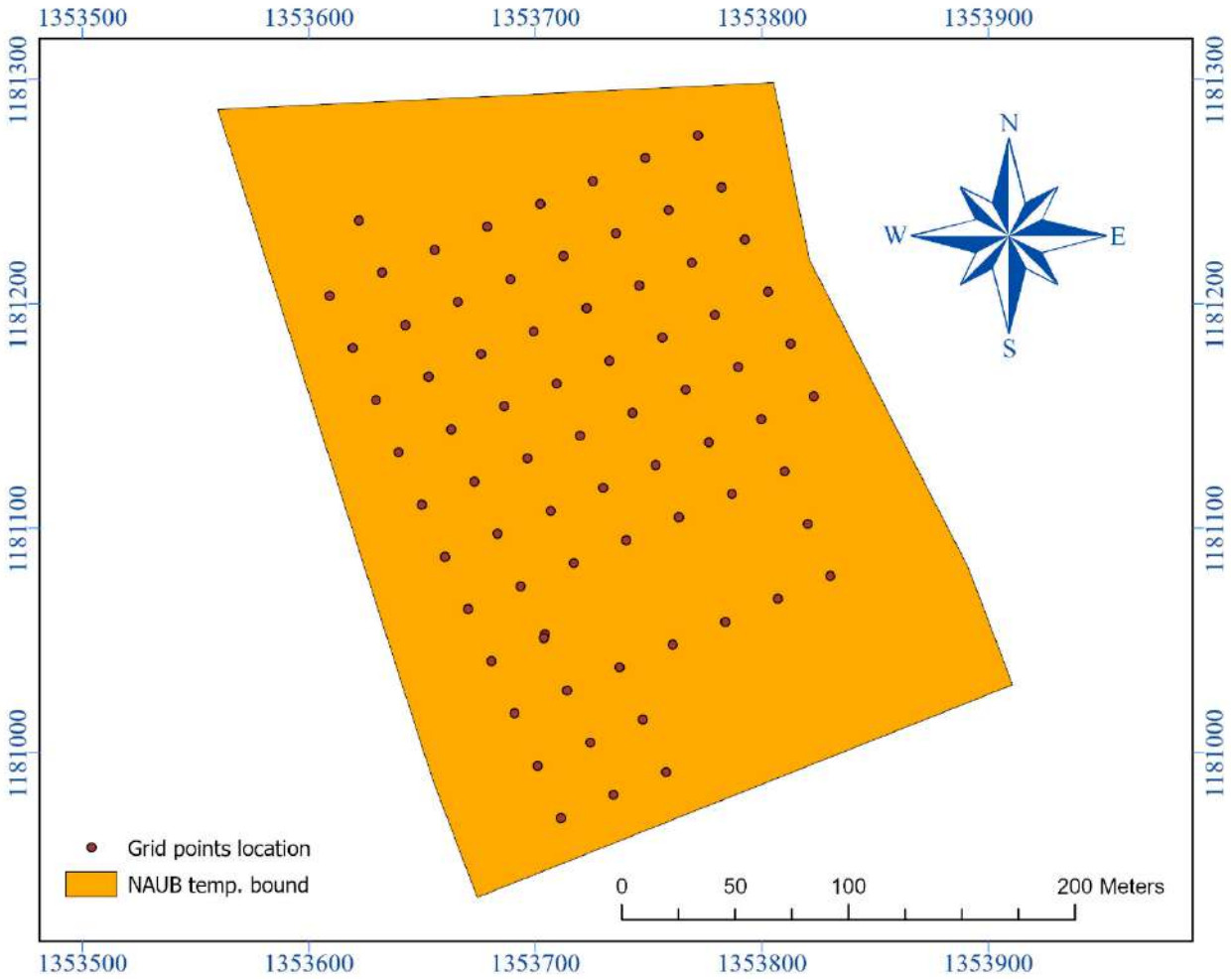

Figure 3: showing Gridded plan of the study site

3.1.2 Google Earth–Derived Spatial Data

The processed Google Earth–derived coordinates were successfully converted and visualized using the GPS Visualizer platform, generating geographic (latitude and longitude), projected (UTM easting and northing), and elevation (altitude) information for the study area Figure 4. The output dataset, extracted as a text file, contains spatial attributes including point type, geographic coordinates, UTM Zone 33P, easting, northing, and elevation values expressed in meters above mean sea level. The results show that the elevation values obtained from Google Earth range approximately between 717 m and 722 m, indicating a relatively gentle topography across the study area. This limited variation in elevation suggests that the terrain is mildly undulating, which is consistent with the physical characteristics observed during field reconnaissance. Such terrain conditions are typical of semi-flat landscapes and are suitable for preliminary planning and reconnaissance-level mapping.

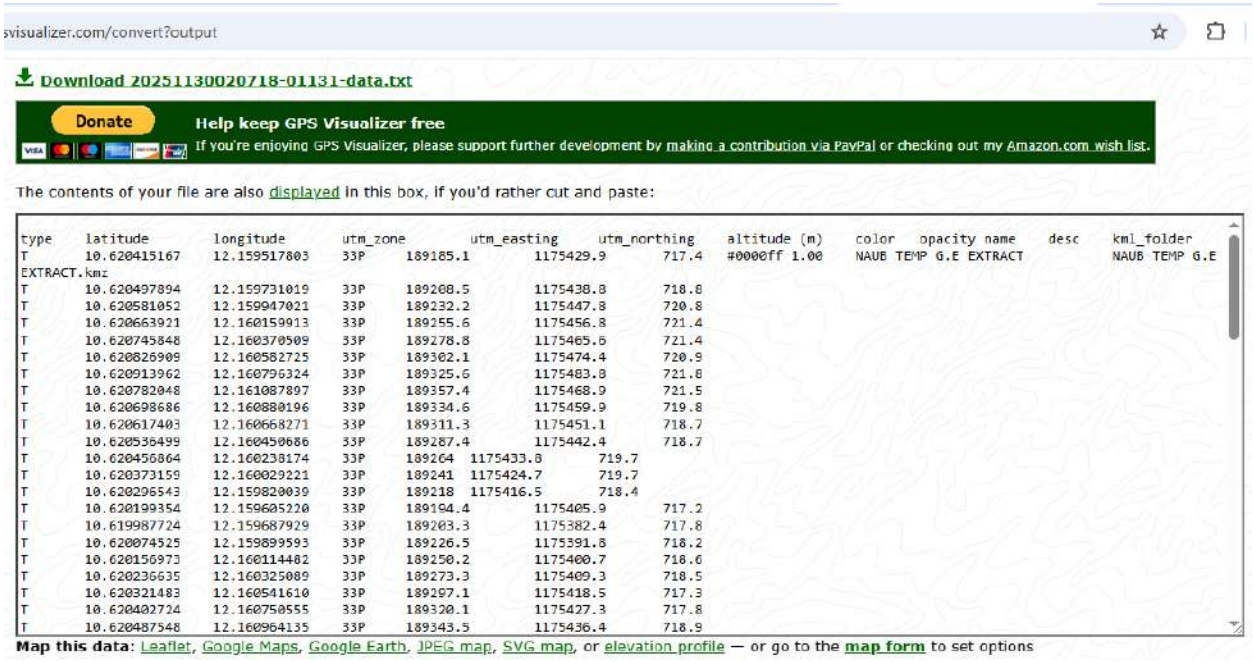
svisualizer.com/convert?output

Download 20251130020718-01131-data.txt

Donate Help keep GPS Visualizer free

If you're enjoying GPS Visualizer, please support further development by making a contribution via PayPal or checking out my Amazon.com wish list.

The contents of your file are also displayed in this box, if you'd rather cut and paste:

type	latitude	longitude	utm_zone	utm_easting	utm_northing	altitude (m)	color	opacity	name	desc	kml_folder
T	10.620415167	12.159517803	33P	189185.1	1175429.9	717.4	#0000ff	1.00	NAUB TEMP G.E EXTRACT		NAUB TEMP G.E EXTRACT.kmz
T	10.620497894	12.159731019	33P	189208.5	1175438.8	718.8					
T	10.620581052	12.159947021	33P	189232.2	1175447.8	720.8					
T	10.620663921	12.160159913	33P	189255.6	1175456.8	721.4					
T	10.620745848	12.160370509	33P	189278.8	1175465.6	721.4					
T	10.620826909	12.160582725	33P	189302.1	1175474.4	720.9					
T	10.620913962	12.160796324	33P	189325.6	1175483.8	721.8					
T	10.620782048	12.161087897	33P	189357.4	1175468.9	721.5					
T	10.620698686	12.160880196	33P	189334.6	1175459.9	719.8					
T	10.620617403	12.160668271	33P	189311.3	1175451.1	718.7					
T	10.620536499	12.160450686	33P	189287.4	1175442.4	718.7					
T	10.620456864	12.160238174	33P	189264	1175433.8	719.7					
T	10.620373159	12.160029221	33P	189241	1175424.7	719.7					
T	10.620296543	12.159820039	33P	189218	1175416.5	718.4					
T	10.620199354	12.159605220	33P	189194.4	1175405.9	717.2					
T	10.619987724	12.159687929	33P	189203.3	1175382.4	717.8					
T	10.620074525	12.159899593	33P	189226.5	1175391.8	718.2					
T	10.620156973	12.160114482	33P	189250.2	1175400.7	718.6					
T	10.620236635	12.160325089	33P	189273.3	1175409.3	718.5					
T	10.620321483	12.160541610	33P	189297.1	1175418.5	717.3					
T	10.620402724	12.160750555	33P	189320.1	1175427.3	717.8					
T	10.620487548	12.160964135	33P	189343.5	1175436.4	718.9					

Map this data: Leaflet, Google Maps, Google Earth, JPEG map, SVG map, or elevation profile — or go to the map form to set options

Figure 4: GPS Visualizer-converted coordinates.

3.1.3 GNSS RTK Survey Observations

The GNSS survey data were processed and organized in Microsoft Excel, as shown in the RTK observation output, Figure 5. The dataset comprises point identifiers, projected coordinates (Easting and Northing), ellipsoidal heights, antenna height, positional precision indicators (σN, σE, σZ), observation time, solution status, and satellite information. The results indicate that the majority of observed points were obtained under RTK Fixed solution status, with a few observations recorded as RTK Float and DGPS. RTK Fixed solutions are characterized by centimeter-level positional accuracy, confirming the reliability and robustness of the GNSS measurements for precise topographic applications. The limited occurrence of RTK Float and DGPS solutions may be attributed to temporary satellite geometry degradation, signal obstruction, or baseline limitations during observation periods. The Easting and Northing coordinates exhibit consistent spatial distribution across the study area, reflecting proper control establishment and stable receiver performance throughout the survey. The recorded ellipsoidal heights show minimal fluctuation within short spatial intervals, further supporting the suitability of the GNSS data for accurate elevation modelling, contour generation, and surface representation.

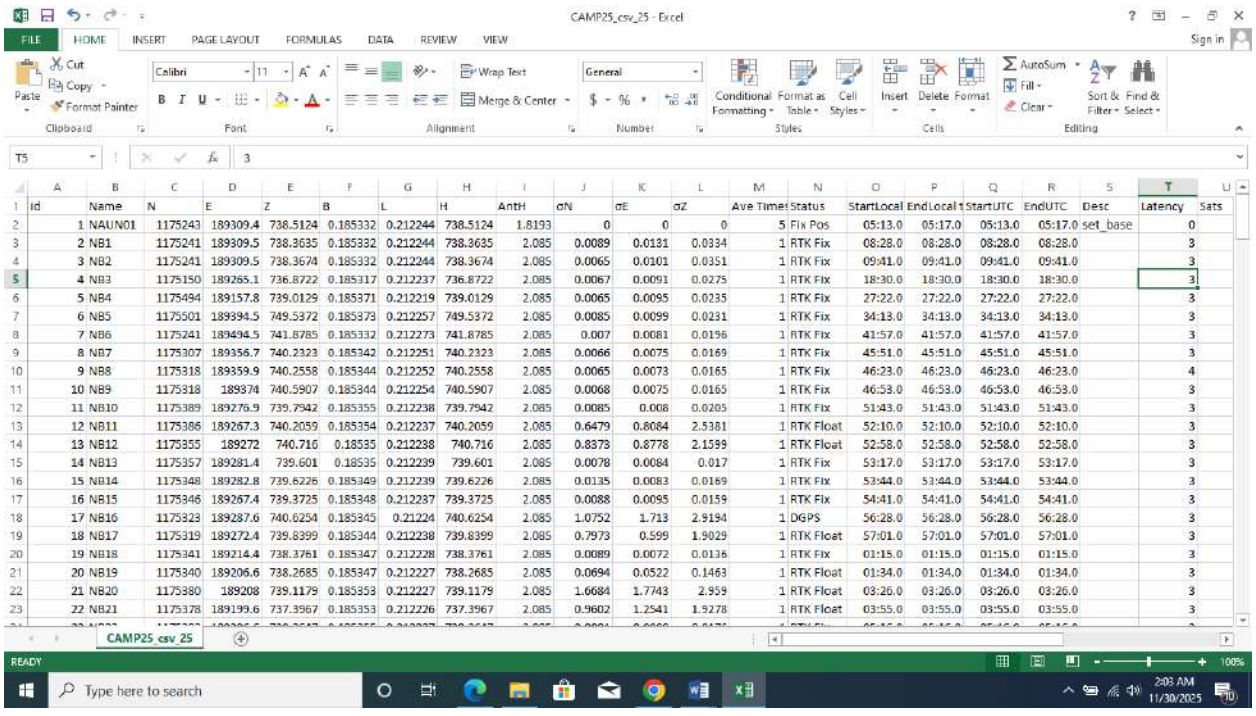

id	Name	N	E	Z	B	L	H	AntH	σN	σE	σZ	Ave Time	Status	StartLocal	EndLocal	StartUTC	EndUTC	Desc	Latency	Sats
1	NAUN01	1175243	189309.4	738.5124	0.185332	0.212244	738.5124	1.8193	0	0	0	5	Fix Pos	05:13.0	05:17.0	05:13.0	05:17.0	set_base	0	
2	NB1	1175241	189309.5	738.3635	0.185332	0.212244	738.3635	2.085	0.0089	0.0131	0.0334	1	RTK Fix	08:28.0	08:28.0	08:28.0	08:28.0		3	
3	NB2	1175241	189309.5	738.3674	0.185332	0.212244	738.3674	2.085	0.0065	0.0101	0.0351	1	RTK Fix	09:41.0	09:41.0	09:41.0	09:41.0		3	
4	NB3	1175150	189265.1	736.8722	0.185317	0.212237	736.8722	2.085	0.0067	0.0091	0.0275	1	RTK Fix	18:30.0	18:30.0	18:30.0	18:30.0		3	
5	NB4	1175494	189157.8	739.0129	0.185371	0.212219	739.0129	2.085	0.0065	0.0095	0.0235	1	RTK Fix	27:22.0	27:22.0	27:22.0	27:22.0		3	
6	NB5	1175501	189394.5	749.5372	0.185373	0.212257	749.5372	2.085	0.0085	0.0099	0.0231	1	RTK Fix	34:13.0	34:13.0	34:13.0	34:13.0		3	
7	NB6	1175241	189494.5	741.8785	0.185332	0.212273	741.8785	2.085	0.007	0.0081	0.0196	1	RTK Fix	41:57.0	41:57.0	41:57.0	41:57.0		3	
8	NB7	1175307	189356.7	740.2323	0.185342	0.212251	740.2323	2.085	0.0066	0.0075	0.0169	1	RTK Fix	45:51.0	45:51.0	45:51.0	45:51.0		3	
9	NB8	1175318	189359.9	740.2558	0.185344	0.212252	740.2558	2.085	0.0065	0.0073	0.0165	1	RTK Fix	46:23.0	46:23.0	46:23.0	46:23.0		4	
10	NB9	1175318	189374	740.5907	0.185344	0.212254	740.5907	2.085	0.0068	0.0075	0.0165	1	RTK Fix	46:53.0	46:53.0	46:53.0	46:53.0		3	
11	NB10	1175389	189276.9	739.7542	0.185355	0.212238	739.7542	2.085	0.0085	0.008	0.0205	1	RTK Fix	51:43.0	51:43.0	51:43.0	51:43.0		3	
12	NB11	1175386	189267.3	740.2059	0.185354	0.212237	740.2059	2.085	0.6479	0.8084	2.5381	1	RTK Float	52:10.0	52:10.0	52:10.0	52:10.0		3	
13	NB12	1175355	189272	740.716	0.18535	0.212238	740.716	2.085	0.8373	0.8778	2.1599	1	RTK Float	52:58.0	52:58.0	52:58.0	52:58.0		3	
14	NB13	1175357	189281.4	739.601	0.18535	0.212239	739.601	2.085	0.0078	0.0084	0.017	1	RTK Fix	53:17.0	53:17.0	53:17.0	53:17.0		3	
15	NB14	1175348	189282.8	739.6226	0.185349	0.212239	739.6226	2.085	0.0135	0.0083	0.0169	1	RTK Fix	53:44.0	53:44.0	53:44.0	53:44.0		3	
16	NB15	1175346	189267.4	739.3725	0.185348	0.212237	739.3725	2.085	0.0088	0.0095	0.0159	1	RTK Fix	54:41.0	54:41.0	54:41.0	54:41.0		3	
17	NB16	1175323	189287.6	740.6254	0.185345	0.21224	740.6254	2.085	1.0752	1.713	2.9194	1	DGPS	56:28.0	56:28.0	56:28.0	56:28.0		3	
18	NB17	1175319	189272.4	739.8399	0.185344	0.212238	739.8399	2.085	0.7973	0.599	1.9029	1	RTK Float	57:01.0	57:01.0	57:01.0	57:01.0		3	
19	NB18	1175341	189214.4	738.3761	0.185347	0.212228	738.3761	2.085	0.0089	0.0072	0.0136	1	RTK Fix	01:15.0	01:15.0	01:15.0	01:15.0		3	
20	NB19	1175340	189206.6	738.2685	0.185347	0.212227	738.2685	2.085	0.0694	0.0522	0.1463	1	RTK Float	01:34.0	01:34.0	01:34.0	01:34.0		3	
21	NB20	1175380	189208	739.1179	0.185353	0.212227	739.1179	2.085	1.6684	1.7743	2.959	1	RTK Float	03:26.0	03:26.0	03:26.0	03:26.0		3	
22	NB21	1175378	189199.6	737.3967	0.185353	0.212226	737.3967	2.085	0.9602	1.2541	1.9278	1	RTK Float	03:55.0	03:55.0	03:55.0	03:55.0		3	

Figure 5: Global Navigation Satellite System (Hi-target GPS) RTK Survey Observations

3.1.4 Conversion from Ellipsoidal to Orthometric Heights

The sample conversion from ellipsoidal heights to orthometric heights Figure 6: Global Navigation Satellite System (Hi-target GPS) RTK Survey Observations was carried out using the UTM coordinate framework on the GRS80 ellipsoid and referenced to the ITRF2020 datum. The results, as presented for selected stations (R002, SUR1, SUR2, and SUR4), demonstrate the practical application of geoid modelling in transforming GNSS-derived heights into physically meaningful elevations above the geoid. The ellipsoidal heights obtained from GNSS observations range between 715.516 m and 729.468 m, while the corresponding derived orthometric heights range from 697.062 m to 711.025 m. The observed differences between ellipsoidal and orthometric heights, representing the geoid undulation, vary consistently across the stations, with values of approximately 18.4 m. This consistency indicates a stable geoid surface within the study area and confirms the reliability of the applied geoid model. The results further show that stations with higher ellipsoidal heights also exhibit proportionally higher orthometric heights, reflecting a uniform vertical transformation across the dataset. This linear relationship validates the mathematical expression H=h−N, H =, where H is the orthometric height, h is the ellipsoidal height, and N is the geoid undulation.

UTM Grid, GRS80 Ellipsoid, ITRF2020

Station	East (m)	North (m)	Zone	Ellipsoidal Height (m)	Derived Above Geoid Height(m)
R002	188640.502	1174115.673	33	718.707	700.251
SUR1	188998.470	1173827.773	33	715.516	697.062
SUR2	188776.842	1173915.431	33	715.521	697.065
SUR4	189261.495	1174813.097	33	729.468	711.025

Figure 6: conversion from Ellipsoidal to Orthometric Heights

3.2 Digital Elevation Model Generation (DEM)

The Digital Elevation Model produced from the DGPS Hi-Target V30 shows a clear and coherent representation of the terrain across the NAUB temporary site, with each colour class depicting a well-structured elevation band that aligns naturally with the field-observed topography. The light blue zone Figure 7 Conversion from Ellipsoidal to Orthometric Heights, representing the lowest elevations between 736.82 m and 739.02 m, spreads smoothly across the western and central portions of the area, forming continuous depressions where surface runoff is likely to collect. This

gently rises into the blue-green elevation band (739.02-741.22 m), which extends evenly around the depression zones and reinforces the gradual slope transitions typical of the site. The green class (741.22-743.41 m) captures the mid-slope surfaces and appears consistently across the central and southeastern regions, providing a stable transition between lower and higher reliefs. Above this, the purple elevation range (743.41-745.61 m) occupies the northeastern segment, forming a compact high-ground area that follows the expected slope orientation. The highest elevations between 745.61 m and 747.81 m are shown in orange concentrated along the eastern boundary where the terrain reaches its natural crest. These colour zones appear continuous, well-structured, and free from fragmentation, demonstrating that the DGPS-derived DEM accurately represents micro-topographic variation and benefits from the centimeter-level precision of the Hi-Target RTK measurements.

However, the DGPS DEM maintains this natural and reliable pattern of terrain representation, the Google Earth DEM-classified using the same colour scheme and elevation ranges exhibits irregular spatial behavior due to the lower resolution and inherent interpolation uncertainty of global elevation datasets. The light blue low-elevation surfaces appear as scattered patches rather than forming a consistent depression, reflecting vertical noise in the Google Earth elevation source. The blue-green and green elevation zones occupy inconsistent and fragmented positions that do not correspond with the DGPS terrain flow, indicating generalized height estimations that are unable to capture local variations. The purple high-ground surfaces are broken and spatially displaced, deviating from the continuous slope pattern recorded in the DGPS data. Similarly, the orange/red highest elevation surfaces appear in locations that do not reflect the true ground peaks, further highlighting the limitations of Google Earth-derived heights for detailed analysis. This contrast in colour distribution and spatial coherence between both DEMs demonstrates that, although Google Earth provides a convenient and accessible elevation source for reconnaissance-level assessment, it lacks the precision required for engineering design, drainage modeling, road alignment, and other applications where accurate local terrain representation is essential. The DGPS-derived DEM therefore stands out as the more reliable dataset and should be adopted as the benchmark for all subsequent analyses within the study.

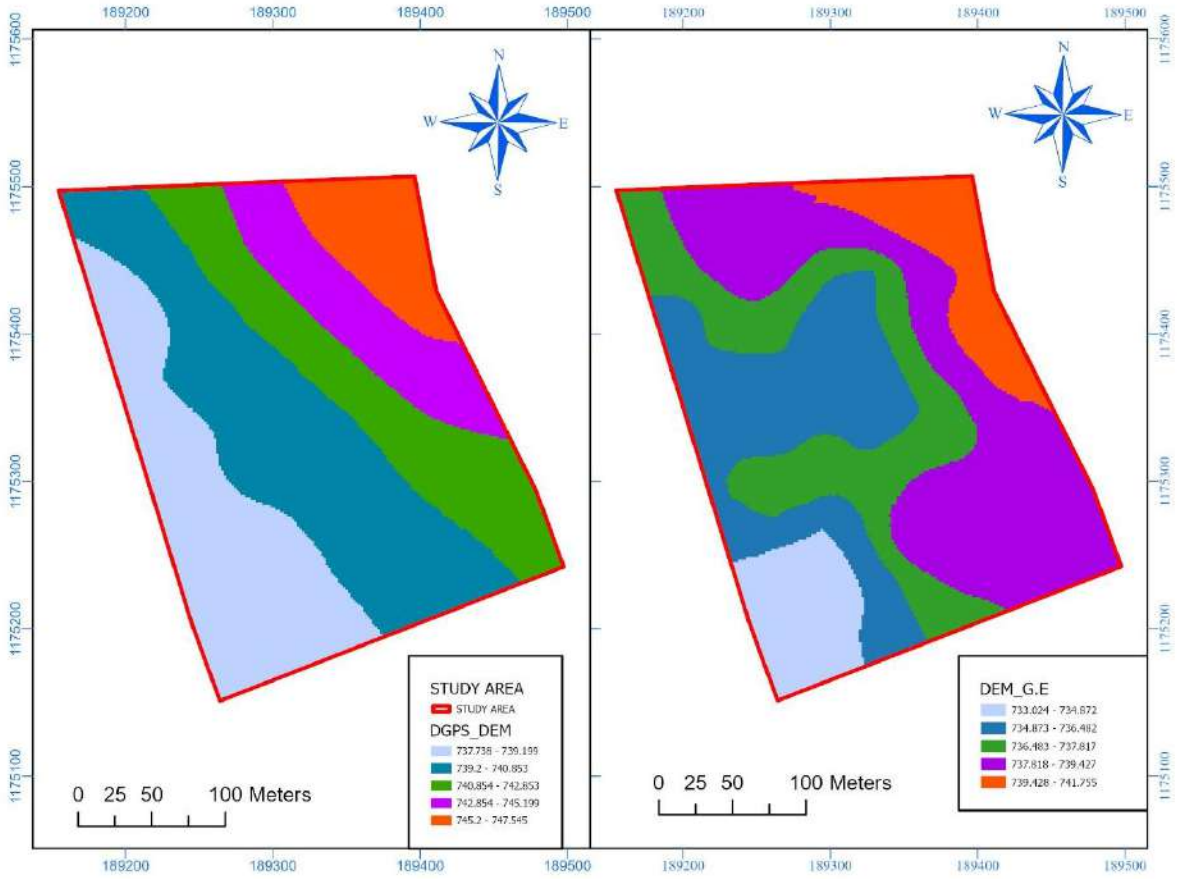

Figure 7**:** DEM produced from DGPS observations (left) and corresponding Google Earth based DEM (right).

3.3 Triangulated Irregular Network (TIN) Comparison

The Triangulated Irregular Network (TIN) surface generated from the DGPS Hi-Target V30 dataset provides a highly detailed and realistic representation of the local terrain within the Nigerian Army University Biu temporary site, Figure 8. The elevation classes are distinctly mapped across the study area, with the yellow zone (710.34-716.25 m) forming the broadest and lowest surface, dominating the southwestern portion of the area and representing gentle depressions that correspond to natural low-lying topography. This smoothly transitions into the green class (716.25-718.16 m), which spreads consistently across the central section of the plot, indicating a gradual rise from the depression and capturing the intermediate elevation surfaces with high spatial accuracy. The purple elevation band (718.16-719.47 m) forms a prominent mid-slope region that aligns naturally with the

expected terrain flow, extending diagonally from the southern to the northeastern part of the area. Above this, the red zone (719.47-720.78 m) marks a steeper elevation rise and occupies the upper central boundary, showing a well-defined and continuous high-ground surface. The highest zone represented by blue (720.78-723.76 m) appears along the northern boundary, forming a compact crest that reflects the true peak elevation measured in the field. These smooth, coherent, and directionally aligned colour transitions confirm the precision of the DGPS-derived TIN, depicting the terrain surface with minimal noise and demonstrating high geometric integrity.

Conversely, the DGPS TIN maintains a natural, well-structured slope pattern, the Google Earth TIN constructed using the same elevation classes' displays irregularities that reflect inconsistencies typical of satellite-derived elevation data. The yellow low-elevation zone appears fragmented and occupies smaller, scattered pockets rather than forming a broad, continuous depression. The green class is distributed in irregular patches that do not correspond with the DGPS terrain structure, producing abrupt elevation shifts that suggest interpolation artifacts. The purple mid-elevation surfaces dominate unexpected sections of the map and appear more uneven, forming shapes unaligned with the natural slope continuity observed in the DGPS TIN. Likewise, the red higher-elevation zone spreads across locations that differ significantly from the DGPS-defined high-ground areas, showing displacement in both vertical and horizontal dimensions. The blue highest elevation class, instead of forming a distinct and compact crest, appears stretched and misplaced relative to the true terrain peaks. These distortions reveal the limitations of Google Earth TIN models, which rely on lower-resolution DEM sources such as SRTM that cannot resolve micro-topographic variations within local-scale project sites. Consequently, although Google Earth TINs are useful for preliminary reconnaissance and general landscape interpretation, the DGPS-derived TIN provides a far more accurate terrain structure suitable for engineering design, drainage assessment, road alignment, and precise geospatial analysis.

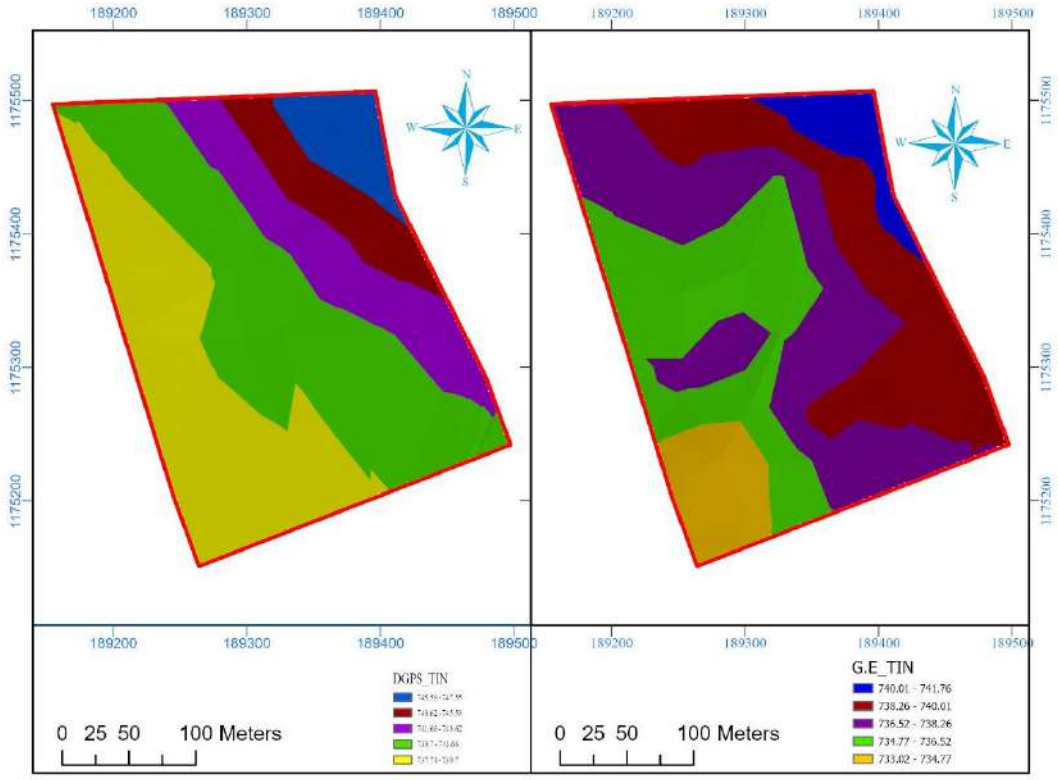

Figure 8**:** Triangulated Irregular Network produced from DGPS data (left) and TIN surface produced from Google Earth (right).

3.4 Contours maps comparison

The contour lines generated from the DGPS Hi-Target V30 dataset, using a 0.5 m contour interval, provide a smooth, coherent, and accurate representation of the terrain at the Nigerian Army University Biu temporary site, Figure 9**.** The contours reveal gradual slope transitions, with wider spacing across the southwestern and central areas indicating gentle slopes and lower elevations, while tighter spacing toward the northeastern and eastern sections reflects rising terrain and consistent slope gradients. The contour shapes are continuous and natural, capturing subtle undulations, minor ridges, and depression basins, demonstrating the precision of RTK-based height measurements and suitability for engineering analyses such as road alignment, drainage, and slope evaluation.

In contrast, Google Earth-derived contours appear irregular, fragmented, and excessively dense in certain areas, suggesting abrupt elevation changes that do not exist on-site. The jagged and cluttered patterns result from coarse-resolution global DEM data, leading to noise-induced distortions, misplaced summit and depression contours, and inconsistencies with true terrain conditions. These discrepancies limit Google Earth contours' applicability for precise surveying and engineering purposes. Overall, the DGPS-derived contour dataset, with its uniform spacing, clear alignment, and reliable representation of micro-topography, provides a highly accurate and interpretable topographic model, making it the definitive source for detailed terrain analysis within the study area.

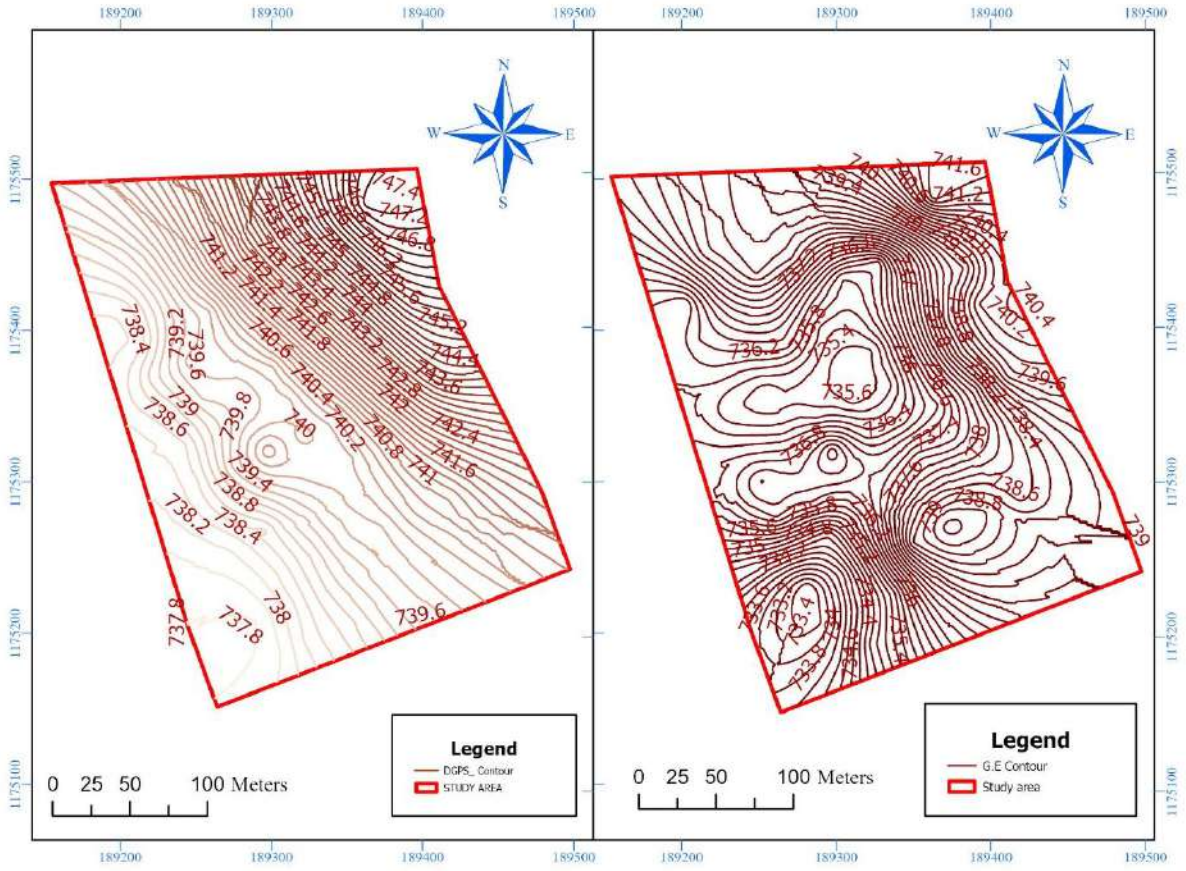

Figure 9: DGPS contour generated from (left) and Google Earth contour generated from (right).

3.5 Statistical Analysis of Elevation Data

3.5.1 Correlation Analysis

The concept of correlation analysis provides a method for measuring the relationship between quantitative variables, categorized as dependent and independent. This relationship is compared using the correlation coefficient (r), which serves as a standardized measure of linear association between variables. The correlation between two sets of measured variables can be either positive or negative, depending on their relationship. It is considered positive when an increase (or decrease) in one variable corresponds to an increase (or decrease) in the other. Conversely, it is negative when an increase in one variable corresponds to a decrease in the other, and vice versa.

The strength of the relationship is expressed through the coefficient of correlation, with values ranging from -1, indicating perfect negative correlation, to +1, indicating perfect positive correlation. In this study, correlation analysis was performed using Microsoft Excel, with the field survey elevation data as the independent variable and the Google Earth data as the dependent variable.

3.5.2 Height Difference Calculation

The elevation difference between GNSS and Google Earth data at each control point was computed to assess the level of agreement between the two datasets.

3.5.3 Descriptive Statistical Analysis

3.5.3.1 Statistical Assessment of Height Differences

The calculated elevation differences were analyzed using key statistical metrics, including the mean, standard deviation, minimum, maximum, and Root Mean Square Error (RMSE). These metrics provide insights into the accuracy, precision, and variability of Google Earth elevation data compared to GNSS measurements table 4 and 5

3.5.3.2 Correlation Analysis between GNSS and Google Earth Heights

A correlation coefficient of 0.701 was obtained, indicating a moderate positive correlation between GNSS-derived heights and those from Google Earth. This suggests a consistent relationship between the two datasets, though some discrepancies exist.

Table 4: Descriptive Statistics:

Description statistics	DGPS Heights(m)	Google Earth (m)
Mean	724.33	718.86
Std deviation	1.79	1.57
Range	720.44,731.23	714.80, 727.00

Table 5: Residuals (Height Differences):

S/no	Statistics analysis	Height diff.
1.	Mean residual	5.47
2.	Std dev. of residual	1.42
3.	Range of residual	1.35, 7.83

This calculation quantifies the discrepancy between the two datasets at each location.

3.6 Observations and Interpretation

The results indicate that GNSS-derived elevations are consistently higher than those obtained from Google Earth, with an average discrepancy of 5.47 meters. The variability in the residuals suggests the presence of systematic differences, which may be attributed to factors such as instrument accuracy, differences in reference datums, or interpolation methods used in Google Earth's elevation model as in figure 10

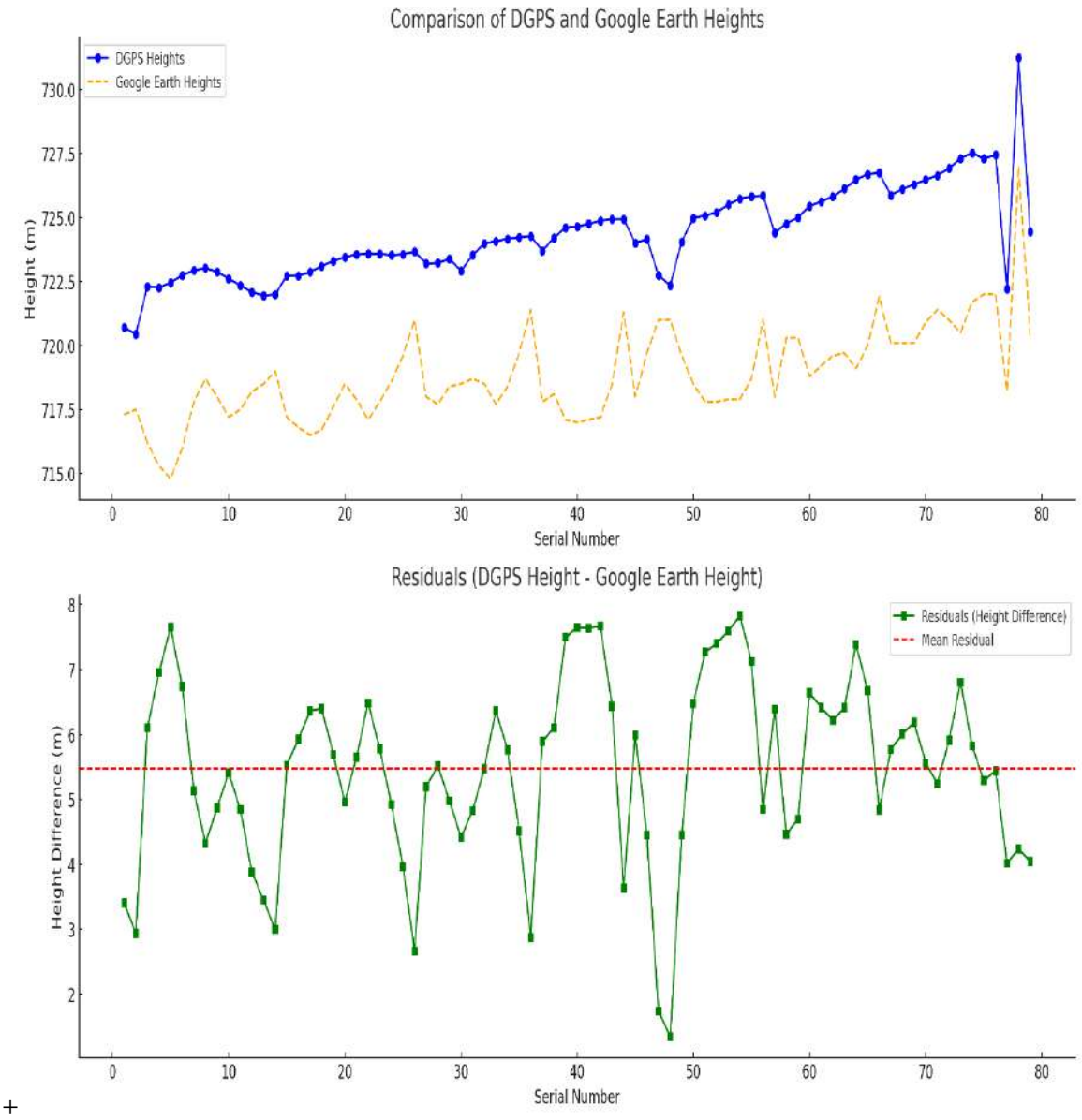

+

Figure 10: showing comparison between Google earth and DGPS

The plot illustrates:

1. **Comparison of DGPS and Google Earth Heights:**

The blue line represents heights obtained using DGPS, while the orange dashed line corresponds to heights from Google Earth. The variations in height values between the two methods are visible across the serial numbers.

2. **Residuals (Height Difference):**

The green line shows the residuals (differences between DGPS and Google Earth heights). The red dashed line marks the mean of the residuals, indicating the average discrepancy.

4.0 CONCLUSION AND RECOMMENDATIONS

4.1 Conclusion

The results showed that GNSS gave a more accurate representation of the terrain with small errors, while Google Earth had larger errors and was less accurate, this comparative study evaluated the positional and vertical accuracy of Google Earth spatial data against high-precision Global Navigation Satellite System (GNSS) measurements at the Nigerian Army University Biu (NAUB) temporary site. By analyzing 72 gridded nodes using both datasets, the research provides a clear perspective on the capabilities and limitations of free, satellite-derived elevation data compared to ground-based surveys.

The investigation reveals a distinct performance gap between the two methods:

a) Precision and Reliability: GNSS measurements, specifically using RTK "Fixed" solutions, consistently delivered centimeter-level accuracy, making them the superior choice for geodetic and engineering applications.
b) Statistical Discrepancies: A moderate positive correlation ($r = 0.701$) was observed between the datasets. However, Google Earth exhibited a systematic vertical bias, with a mean height difference of 5.47 m and a standard deviation of 1.42 m compared to the GNSS reference.
c) Terrain Representation: Spatial models (DEM, TIN, and contours) derived from GNSS provided a smooth, coherent, and realistic depiction of the terrain. In contrast, Google Earth-derived models appeared fragmented and "noisy," often failing to capture micro-topographic variations essential for detailed engineering design.

Ultimately, while Google Earth is a valuable and accessible tool for reconnaissance, preliminary planning, and large-scale site familiarization, it lacks the necessary precision for rigorous

engineering tasks. For projects involving construction design, earthwork volume estimation, or material quantification where errors can lead to significant cost overruns the adoption of GNSS remains essential for ensuring data integrity and project success.

4.2 Recommendations

Base on the result obtained the following recommendations were made

1. Professional and Engineering Practice

   GNSS should be used as the main tool for topographic, engineering, and construction surveys where high accuracy is needed. GNSS data should be used for detailed design, earthwork calculation, road layout, drainage planning, and material estimation to reduce errors that may come from using Google Earth data.

2. Use of Google Earth

   Google Earth is useful for preliminary surveys, planning, and getting an overall view of a site. It can be used for quick mapping and site familiarization, but it should not be used for detailed engineering work or where precise measurements are needed.

3. Future Research

   Future studies should look at combining GNSS with high-resolution satellite data to improve mapping in areas with complex terrain. Research could also explore using new technologies like drones with LiDAR or other sensors to support GNSS data and check if they are cost-effective for surveying, planning, and construction work.

REFERENCES

American Society of Civil Engineers. (2003). Study on accuracy of 1-degree DEM versus topographic map. *Journal of Surveying Engineering*, 129(2), 85–92. https://airccse.com/civej/papers/1114civej02.pdf

Benker, E. M., Gunsch, J. H., & Heermann, P. (2017). Google Earth elevation data extraction and accuracy assessment. PLoS ONE, 12(4), e0175756.

Botygina, N. (2025). *GNSS vs GPS: Understanding the difference in mapping accuracy*. Emlid. https://blog.emlid.com/gnss-vs-gps-understanding-the-difference-in-mapping-accuracy/

BP Chaliha College. (n.d.). Digital elevation model (DEM) in GIS.

Chigbu, O. C., Ayodele, T. O., & Nwafor, O. C. (2019). Comparative analysis of Google Earth derived elevation data. *FIG Working Week 2019 Proceedings*. https://www.fig.net/resources/proceedings/fig_proceedings/fig2019/papers/ts05f/TS05F_chigbu_okezie_et_al_10129.pdf

Civil Engineering Journal Editorial Office. (2024). Assessing geospatial accuracy in mapping applications. *Civil Engineering Journal*. (*Volume and issue numbers)* https://www.civilejournal.org/index.php/cej/article/download/5097/pdf/13796

El-Ashmawy, K. L. A. (2024). Vertical accuracy of Google Earth data. *Engineering, Technology & Applied Science Research*, 14(3), 13830–13836. https://doi.org/10.48084/etasr.7121

Fisher, P. F., Tate, N. J., & Wang, Q. (2010). Impact of DEM accuracy and resolution on topographic indices. *Environmental Modelling & Software*, 25(10), 1194–1203. https://doi.org/10.1016/j.envsoft.2010.03.014

Guo, J., Wang, S., & Sun, L. (2020). Horizontal accuracy assessment of Google Earth data over typical regions of Asia. *ISPRS Archives*, XLIII-B3, 1333–1338. https://doi.org/10.5194/isprs-archives-XLIII-B3-2020-1333-2020

International Hydrographic Organization. (n.d.). Chapter 6: Topographic surveying. IHO Standards for Hydrographic Surveys. https://iho.int/uploads/user/pubs/cb/c-13/english/C-13_Chapter_6.pdf

Journal of Maps and Spatial Engineering. (n.d.). Positional accuracy testing of Google Earth https://www.ijmse.org/Volume4/Issue6/paper2.pdf

MES Innovation. (2022). How accurate is Google Earth elevation? https://mes100.com/docs/how-accurate-is-google-earth-elevation/

Mesbah, S., Madbouly, M. M., & Ghanem, M. (2023). Error assessment and propagation in digital terrain modeling*: A review*. *The International Archives of the Photogrammetry, Remote Sensing and Spatial Information Sciences, XLVIII-1/W2*, 611–617.

Mettatec. (2023). Topographic survey with total station or with GNSS RTK? https://mettatec.com/topographic-survey-with-total-station-or-with-gnss-rtk/

Nigerian Journal of Environmental Sciences and Technology. (2023). Comparative analysis of the horizontal positional accuracy. *NIJEST*, 6(1), 234–245. https://nijest.com/wp-content/uploads/2023/01/234-245_0341_Vol.-6-No.-1_NIJEST.pdf

Olatunde, F. O., & Olatunde, M. B. (2025). Comparative analysis of GNSS (RTK) and total station-derived results in topographical mapping. *International Journal of Advanced Multidisciplinary Research and Studies*, 5(2), 1376–1382. From https: /doi.o rg/ 10.62225/2583049X.2025.5.2.3989

Omona, S., Kyarisiima, C., & Mugisha, J. (2021). GNSS technology's contribution to topography. *Journal of Geographic Information System*, 13(9), 123–136. https://doi.org/10.4236/jgis.2021.93066

Open Topography. (2023). Interpreting errors in topographic differencing results. https://opentopography.org/blog/interpreting-errors-topographic-differencing-results

Orhan, O., Aydar, U., & Yilmaz, M. (2023). Accuracy assessment of height difference using total station and levelling instrument. *World Scientific News*. https://worldscientificnews.com/accuracy-assessment-of-height-difference-using-total-station-and-levelling-instrument/

Potuckova, M., Karas, J., & Ruzicka, J. (2020). Horizontal accuracy assessment of Google Earth data. *ISPRS Archives*, XLIII-B3, 1333–1338 https://isprs-archives.c opernicus .org/articles/XLIII-B3-2020/1333/2020/

Richard, O. (2017). Analysis of accuracy of differential global positioning system. FIG Working Week 2017 Proceedings. https:/ /www.fi g.net/res ources/pr oceedings/ fig_procee dings /fig20 17/papers/ts08c/TS08C_richard_ogba_8585.pdf

Sensors and Materials Editorial Office. (2023). Accuracy assessment of Google Earth and open-source digital elevation models. *Sensors and Materials*, 35(9). https://doi.org/10.18494/SAM4394

Sharma, A., & Gupta, D. (2014). Derivation of topographic map from elevation data available in Google Earth. Civil Engineering and Urban Planning: *An International Journal* (CiVEJ), 1(1), 14.

Tishk International University (2021). Surveying with GNSS and total station: A comparative study. Eurasian Journal of Applied Sciences and Engineering. https://eajse.tiu.edu.iq/index.php/eajse/article/view/184

University of Baghdad. (n.d.). GNSS positioning techniques for enhancing Google Earth imagery. https://repository.uobaghdad.edu.iq/articles/hxeSapIBVTCNdQwC268d

World Scientific News. (n.d.). Accuracy assessment using total station. https://worldscientificnews.com/